Neuron, Vol. 29, 519–527, February, 2001, Copyright ©2001 by Cell Press

Orientation Preference Patterns in Mammalian Visual Cortex: A Wire Length Minimization Approach

Alexei A. Koulakov* and Dmitri B. Chklovskii†‡
*The Salk Institute
10010 North Torrey Pines Road
La Jolla, California 92037
†Cold Spring Harbor Laboratory
1 Bungtown Road
Cold Spring Harbor, New York 11724

Summary

In the visual cortex of many mammals, orientation preference changes smoothly along the cortical surface, with the exception of singularities such as pinwheels and fractures. The reason for the existence of these singularities has remained elusive, suggesting that they are developmental artifacts. We show that singularities reduce the length of intracortical neuronal connections for some connection rules. Therefore, pinwheels and fractures could be evolutionary adaptations keeping cortical volume to a minimum. Wire length minimization approach suggests that interspecies differences in orientation preference maps reflect differences in intracortical neuronal circuits, thus leading to experimentally testable predictions. We discuss application of our model to direction preference maps.

Introduction

Neurons in mammalian visual cortex respond best to edges in their receptive field. Edge orientation, which evokes most vigorous response, determines orientation preference of a neuron. Electrophysiological studies have shown that preferred orientation remains constant in vertical penetrations while varying in the directions parallel to the cortical surface (Hubel and Wiesel, 1974). Two-dimensional maps of preferred orientation were revealed electrophysiologically (Swindale et al., 1987) and optically (Bonhoeffer and Grinvald, 1991; Blasdel, 1992). Further research showed significant differences in map appearance between species. In visual cortices of monkeys, ferrets, tree shrews, and cats, the maps contain linear zones, where orientation preference changes smoothly. These linear zones are periodically interspersed by pinwheels, i.e., point singularities, and fractures, i.e., line discontinuities. Recently, optical imaging in tree shrews (Bosking et al., 1997) and cats (Shmuel and Grinvald, 2000) showed extensive pinwheel-free linear zones, i.e., *Icecube* regions. Electrophysiology in rats shows that nearby neurons have different preferred orientation, indicating a *Salt&Pepper* layout (Girman et al., 1999).

In order to account for orientation preference maps, a variety of models (Erwin et al., 1995; Swindale, 1996) were proposed. Many of these models reproduced orientation preference map of realistic appearance. However, the reason for the existence of singularities in the maps and the variability in the map structure has remained elusive. Analysis of a representative model (Swindale, 1982; Cowan and Friedman, 1991) based on lateral inhibition, which could result from competitive Hebbian learning, shows that the ultimate orientation preference map that minimizes the corresponding cost-function does not contain singularities and is instead given by the *Icecube* layout (see Experimental Procedures). Therefore, in the framework of these models, pinwheels and fractures result from imperfect development reflected in incomplete cost-function minimization.

Hubel and Wiesel (1977) suggested that orientation preference maps result from evolutionary pressure to minimize cortical wire length while maximizing coverage. This suggestion inspired dimension reduction approach, which was implemented by elastic net models (Durbin and Mitchison, 1990; Goodhill and Cimponeriu, 2000). These models also produce maps of realistic appearance, including pinwheels in orientation map. However, elastic net models seem to predict annihilation of pinwheels (Wolf and Geisel, 1998), suggesting that *Icecube* layout is the ultimate state and pinwheels are developmental defects.

In this paper, we prove that singularities are required by an evolutionary principle. We compare the wire length for smooth and discontinuous maps and show that singularities reduce the brain volume in some cases. Our theory reproduces interspecies variability in map structure and relates it to experimentally measurable properties of intracortical neuronal circuits.

We base our model on wire length minimization principle (Allman and Kaas, 1974; Cowey, 1979; Nelson and Bower, 1990; Mitchison, 1991; Cherniak, 1994; Cajal, 1999; Chklovskii and Stevens, 1999; Chklovskii and Koulakov, 2000). Since axons and dendrites take up a significant fraction (about 60%) of the cortical volume (Braitenberg and Schüz, 1998), limitations on the brain size require keeping neuronal processes as short as possible. Evolution was likely to select for developmental rules that produce sufficiently optimized, in terms of wire length, orientation maps. Therefore, we attempt to reproduce orientation preference maps by minimizing the length of neuronal connections, or wiring.

To formulate the model, we notice that the majority of inputs received by cortical neurons come from local connections, which stay within the cortex (LeVay and Gilbert, 1976; Peters and Payne, 1993; Ahmed et al., 1994), rather than from thalamocortical projections. Therefore, we look for the neuronal layout that minimizes the length of intracortical wiring. We assume that intracortical connections can be described by a connection function, $c(\theta)$. This function gives the number of connections a neuron establishes with other neurons whose orientation preference differs by θ. Based on anatomical (Buzas et al., 1998; Roerig and Kao, 1999; Yousef et al., 1999), electrophysiological (Gardner et al., 1999), and psychophysical (Lee et al., 1999) observations, we express the connection function as a sum of Gaussian

‡To whom correspondence should be addressed (e-mail: mitya@cshl.org).

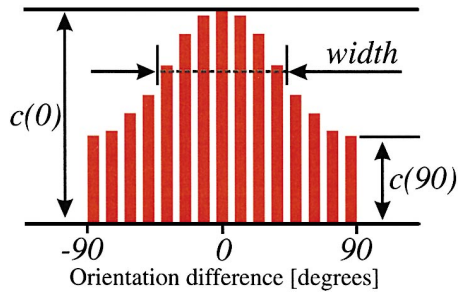

Figure 1. Parameters of the Connection Function

Bars represent numbers of connections that each neuron must receive from neurons with different orientation preferences.

and constant components. We study how optimal layout depends on the two parameters of the connection function: the width of the Gaussian and the relative magnitude of the constant component. We obtain a complete phase diagram for these parameters of the connection function.

Results

In our model, the number of connections with neurons whose orientation preference differs by θ is dictated by the connection function:

$$c(\theta) = \left\{ A \sum_{n=-\infty}^{\infty} e^{-\frac{(\theta - 180^\circ \cdot n)^2}{2a^2}} + B \right\}. \quad (1)$$

Here {x} rounds x to the nearest integer, coefficients *A* and *B* determine the magnitude of Gaussian and constant components, respectively. We express the first component as a series of identical Gaussians spaced by 180° in order to keep the connection function smooth at ±90°. The values of the connection function at 90° and 0° are denoted as *c(90)* and *c(0)*, respectively (Figure 1). Since for large numbers of connections [$c(0) \gg 1$] the appearance of the map depends only on the ratio of parameters *c(90)* and *c(0)*, and not on their absolute values, we represent our results as the function of *c(90)/c(0)*.

We consider connection functions whose *width*, as defined in Figure 1, is equal to 10, 14, 20, 35, 49, 60, 82, and 90 degrees. These values are generated by *a* equal to 4, 6, 9, 12, 15, 21, 26, 38, and 66 degrees, respectively. For the values of *a* below 24°, the connection function *width* is related to parameter *a* according to $width = 2a\sqrt{2\ln 2}$ and Equation 1 reduces to the following:

$$c(\theta) = \{[c(0^\circ) - c(90^\circ)]e^{-\theta^2/2a^2} + c(90^\circ)\}. \quad (2)$$

For these connection functions, we look for the layout of neurons on a square lattice that minimizes the total length of connections. The details of the numerical algorithm are given in the Experimental Procedures section. Below we present the results and give an intuitive interpretation.

We start with a purely constant connection function, whereby each neuron is required to establish equal numbers of connections with neurons of all preferred orientations. We find that the optimal layout in this case is the

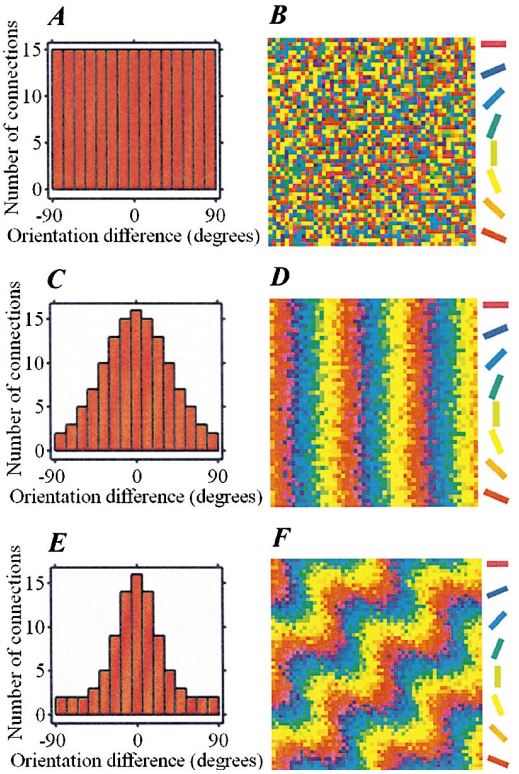

Figure 2. Broad Connection Functions and Corresponding Orientation Maps

Constant connection function (A) and *Salt&Pepper* orientation map (B); (C and D) *Icecube* (width of Gaussian = 82°, c(90)/c(0) = 2/16); (E and F) *Wavy Icecube* (width of Gaussian = 49°, c(90)/c(0) = 2/16). Maps in (B) and (D) represent arrays of 50 × 50 neurons with periodic boundary conditions, whereas the map in (F) shows a 60 × 60 array. For our numerical analysis, we discretize the connection function into 15 preferred orientation classes.

Salt&Pepper arrangement (Figures 2A and 2B). In this layout, neurons of each preferred orientation are equally represented at every location, thus allowing local connections to satisfy fully the requirements of the constant connection function. Note that the constant connection function does not imply that it does not matter which orientation is connected to which. Each neuron in Figure 2B *must* connect to an equal amount of "blue," "red," and "yellow" neurons, for instance. In the Experimental Procedures, we prove that *Salt&Pepper* is the optimal layout for the constant connection function.

Next, for a wide Gaussian, we find numerically that the optimized layout is the *Icecube*, or smooth linear arrangement (Figures 2C and 2D) (*width* of Gaussian = 82°). Peaking of the connection function around zero orientation difference implies more connections between neurons of similar orientation preference, which leads to clustering of neurons of similar orientation preference. In Experimental Procedures, we prove that *Icecube* layout is optimal for the class of semi-elliptic connection functions.

In general, the appearance of the optimal map results from competing requirements of the Gaussian and constant components of the connection function. The Gaussian part of the connection function creates an effec-

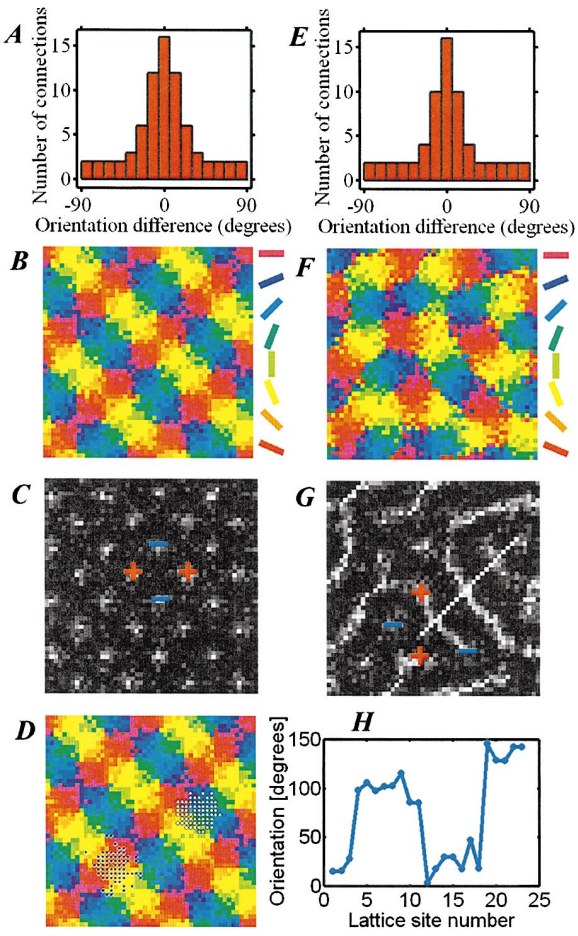

Figure 3. Narrow Connection Functions and Corresponding Orientation Maps

(A–C) *Pinwheels* (width of Gaussian = 35°, c(90)/c(0) = 2/16); (E–G) *Pinwheels and Fractures* (width of Gaussian = 28°, c(90)/c(0) = 2/16). (C) Orientation gradient map. Lighter areas correspond to regions of higher gradient (pinwheels). Four 180° pinwheels are shown by plus and minus signs, which designate the clockwise and counterclockwise change in orientation preference while walking around the pinwheel. (D) shows locations of neurons (circles) connected to a given neuron (crosses). (G) Orientation gradient map. Fractures are bright lines of high gradient. They terminate at 90° pinwheels designated by plus and minus. Notice that the discontinuity of preferred orientation at the fracture is close to 90° (see also [F] and [H]). (H) Preferred orientation along the track shown by the bright line in (G). This line intersects three fractures. The change of the preferred orientation on the first two of them is close to 90°. The variation of orientation on the third is about 100°, after averaging the short-range oscillations on two sides of the fracture.

tive attraction between neurons of similar orientation preferences. Therefore, the Gaussian part favors the *Icecube* arrangement, where orientation changes smoothly from point to point. On the other hand, the constant component of the connection function creates an effective attraction between neurons of unlike preferred orientation. The constant component favors discontinuities in the orientation map, as manifested in the *Salt&Pepper* layout. The relative weight of the two components determines the optimal layout. As the Gaussian narrows, its relative weight diminishes, and singularities start to appear in the optimized map (Figure 3).

When the connection function narrows sufficiently, the optimized layout is a lattice of pinwheels (Figures 3A–3D). This arrangement contains regions where orientation changes smoothly as required by the Gaussian part of the connection function. At the same time, there are singularities where neurons of all possible orientation preferences are present. Hence, a neuron does not have to look farther than the nearest pinwheel to make connections with all orientation preferences as required by the constant part of the connection function.

In the extreme case of a very narrow connection function, the optimized layout consists of linear zones, or *Icecube* patches, separated by fractures terminating on pinwheels (Figures 3E–3H). Linear zones accommodate connections required by the Gaussian part of the connection function. Fractures realize short connections between neurons of dissimilar preferred orientation required by the constant part of the connection function (see, also, Das and Gilbert, 1999).

In the intermediate region between *Icecube* and *Pinwheel* layouts, we find *Wavy Icecube* (Figures 2E and 2F) (Braitenberg and Braitenberg, 1979). Bending of the *Icecube* is the result of attraction between neurons of dissimilar preferred orientations. Again, this layout combines clustering of similarly oriented neurons with bringing orthogonally oriented neurons closer than in a regular *Icecube*.

In addition to varying the width of the Gaussian, we alter the balance between the two components of the connection function by changing the magnitude of the constant component. We represent our results in a phase diagram (Figure 4) that shows optimized layouts as a function of the Gaussian width and the relative strength of constant component of the connection function.

In our model, layouts, other than *Salt&Pepper,* have a characteristic periodic appearance. The period of the layout is determined by the numbers of connections in the $c(\theta)$. The structure of the maps does not change when the connection function is rescaled by a constant factor, while the period of the pattern scales as the square root of the number of connections.

Application of the Model to Direction Preference Maps

Although the current model was developed for orientation preference maps, it can be applied to other cortical maps. For example, as revealed by intrinsic optical imaging, direction preference maps exist in visual cortex of many species. These maps exhibit regions of continuous change in direction preference, separated by occasional fractures where preferred direction changes by 180° (Malonek et al., 1994; Shmuel and Grinvald, 1996; Weliky et al., 1996; Kim et al., 1999).

Results for orientation preference maps presented here can be carried over to direction preference maps, provided connectivity between neurons of different preferred directions can be approximated by a connection function of a central Gaussian and a constant background. To do this, we notice that preferred orientation varies in the range {−90°; 90°}, while preferred direction variable must be in the range {−180°; 180°}. Therefore, we need to rescale all angles by a factor of two both in

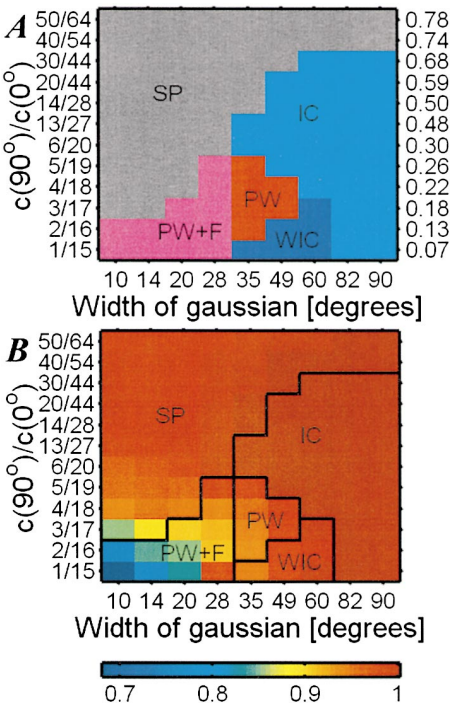

Figure 4. Phase Diagram of Orientation Preference Patterns

(A) Optimized layouts for different values of the Gaussian width at half-height and the ratio between numbers of connection with neurons of the same and orthogonal orientation. SP, *Salt&Pepper*; PW, *Pinwheel*; PW+F, *Pinwheel and Fracture*; IC, *Icecube*; and WIC, *Wavy Icecube*. The column of fractions on the left shows the actual minimum and maximum values of connection function used in calculation. The column on the right shows the decimal representation of these fractions.

(B) Decrease in wire length in optimized maps relative to the optimal *Icecube* layout for a given connection function. The lines show the phase boundaries from (A). The formation of singularities (pinwheels and fractures) for the narrow connection function reduces wire length by more than 30% (lower left corner).

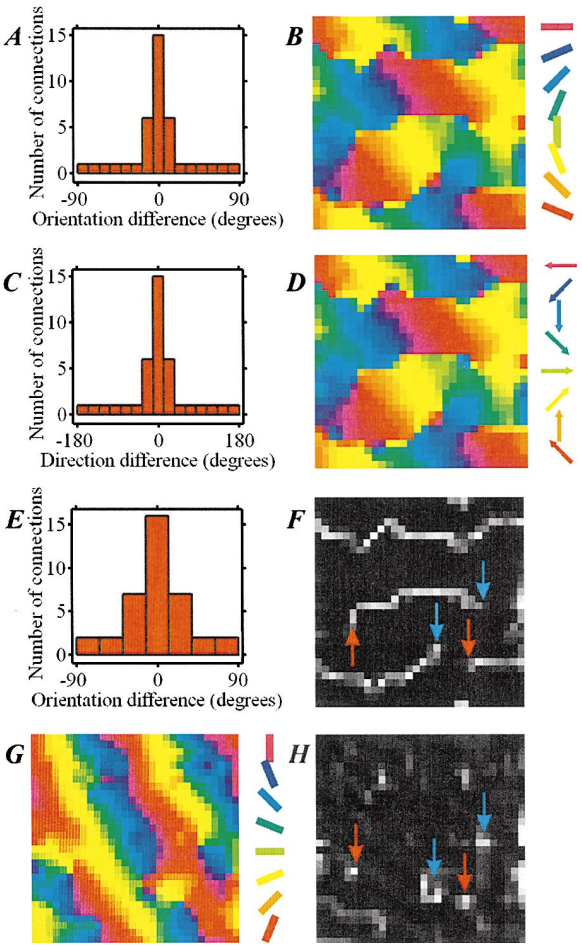

Figure 5. Relation between Orientation and Direction Preference Maps

Orientation connection function (A) and the corresponding orientation preference map (B). Direction connection function (C) and the corresponding direction preference map (D) obtained by simple rescaling of the orientation map. (F) Gradient direction map (lighter pixels reflect higher gradient values) showing fractures terminating at 90° pinwheels (arrows). (E) Orientation connection function describing connections in the direction map (D). Orientation map obtained from the direction map (D) by invoking orthogonality of preferred orientation and preferred direction for a given neuron. (H) Gradient of the orientation map (G). Bright spots are 180° pinwheels.

connection functions and in the maps. An example of the rescaling is shown in Figures 5A–5D for a narrow connection function. The corresponding direction preference map contains linear zones and fractures, where direction preference changes by 180°.

Next, we consider the appearance of the orientation preference map for the same region as described by the direction preference map. To do this, we notice that orientation preference of a given neuron is orthogonal to its direction preference. Therefore, we can obtain the orientation preference map (Figure 5G) from the direction preference map (Figure 5D). The corresponding orientation preference map shows linear regions and pinwheels. The linear regions in orientation map originate from the linear regions in direction map. Fractures in direction map turn into linear regions in orientation map, because when direction changes by 180°, preferred orientation remains the same (Figures 5F and 5H). Finally, terminations of fractures in direction maps produce pinwheels in orientation maps (Figures 5H). This is because the direction preference gradually changes by 180° while going around the termination of the fracture and then jumps by 180° at the fracture. Since preferred orientation is orthogonal to preferred direction, it makes a full 180° circle while going around the termination of the fracture and does not change across the fracture. These direction preference maps are consistent with experimental observations (Malonek et al., 1994; Shmuel and Grinvald, 1996; Weliky et al., 1996; Kim et al., 1999).

Discussion

Comparison with Experimental Observations

The types of orientation preference maps obtained in our model span most of the observed interspecies variability. Below we compare our results with experimentally obtained orientation maps in different species.

The *Salt&Pepper* layout resembles the situation in rat V1, where neurons of all preferred orientations are pres-

ent at every point (Girman et al., 1999). This is despite the fact that each individual neuron is well tuned for orientation.

The situation in rat V1 raises a question about the relation between the tuning of neuronal response and the tuning of the connection function. Although they are related, these two tunings do not have to coincide. This is because contributions of input connections to the tuning of neuronal activity are weighted by the synaptic strength that varies from connection to connection and may even be negative (for inhibitory inputs).

Our model yields layouts with no singularities at all, such as *Icecube* (Figure 2D). *Icecube* arrangements, or linear zones, are common in tree shrews along the V1/V2 border and along the caudal edge of the dorsal portion of V1 (Bosking et al., 1997). Linear zones have recently been observed in sizable regions of cat V2 (Shmuel and Grinvald, 2000). Thus, singularities in orientation maps are not always necessary, in agreement with our predictions.

By comparing our orientation maps with experiments done in cats (Swindale et al., 1987; Bonhoeffer and Grinvald, 1991), monkeys (Blasdel, 1992), and tree shrews (Bosking et al., 1997), we conclude that the orientation map in Figure 3F comes closest to these maps. In particular, we observe linear zones that are segregated by fractures. The change of preferred orientation on these fractures is close to 90° (Figure 3H). This is in accord with the experimental observations. The fractures terminate on 90° pinwheels (Figure 3G). In addition, we obtain standalone 180° pinwheels, which are not connected to any fracture. Both types of singularities are observed in these species.

Good agreement between Figure 3F and the data from cats, monkeys, and tree shrews suggests that the connection function in these species is close to the one shown in Figure 3E. This is consistent with the measurements of the connection function (Roerig and Kao, 1999; Yousef et al., 1999), according to which the central peak has a width of 20°–40°.

The periodic *Pinwheel* layout (Figure 3B) resembles that in ferrets (Weliky et al., 1996) (see, however, Rao et al., 1997). At the same time, the direction map in ferret V1 contains fractures. The relationship between orientation and direction preference maps in our model is discussed in the Results.

The maps observed in ferrets and other mammals are far from regular (Bonhoeffer and Grinvald, 1991; Blasdel, 1992; Bosking et al., 1997). We attribute the irregular arrangement of singularities seen in experimental orientation maps to both developmental noise and to various sorts of quenched disorder, such as the weak coupling between orientation and other maps, the presence of blood vessels, etc. To mimic such variability, we performed an incomplete wire length minimization, limiting the annealing procedure (see Experimental Procedures) to 1,000 steps instead of 10,000. The result of one such incomplete run is shown in Figure 6B. The connection function in Figure 6A corresponds to the region of phase diagram occupied by the lattice of 180° pinwheels. It is evident from Figure 6 that the regularity of pinwheel lattice is destroyed if noise is added to the system. At the same time, the local structure of the map dominated by 180° pinwheels is preserved. This suggests that conclusions of our model are robust with respect to developmental noise and disorder pertinent real maps.

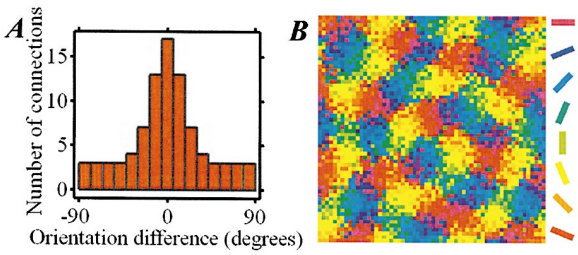

Figure 6. Result of an Incomplete Minimization of the Wire Length

(A) The connection function belongs to the area on the phase diagram corresponding to the lattice of pinwheels (width of Gaussian = 35°, c(90)/c(0) = 3/16).

(B) 60 × 60 array of preferred orientations resulting from only 1/10th of the regular optimization process.

Wolf and Geisel (1998) suggested analyzing cortical orientation maps by comparing the scaled density of pinwheels $\hat{\rho} = n\lambda^2$, where n is the density of pinwheels and λ is the characteristic spacing of iso-orientation domains. The scaled density measures the number of pinwheels in a region of area λ^2. The average values of this quantity vary from 2.1–2.6 in tree shrews to about 3.5 (Obermayer and Blasdel, 1997) or 3.75 (Wolf and Geisel, 1998) in macaque monkey. The average values for other species are between tree shrew and monkey. However, intraspecies variability in macaque monkey is rather high, $3 < \hat{\rho} < 4.5$, as inferred from Obermayer and Blasdel (1997). The scaled density of pinwheels in our model is expected to be smaller or comparable since additional pinwheels may be generated by noise in real system (Wolf and Geisel, 1998). The scaled density for the maps in Figures 3B and 3F is equal to 3.9 and 1.2, respectively. For the incompletely optimized map in Figure 6B, the scaled density is 3.3. Thus, the values of scaled density observed in our model are within the experimentally observed range.

Experimental Predictions

Orientation preference maps vary substantially between species and even within one animal. Wiring optimization hypothesis suggests that these differences reflect variations in intracortical circuitry. In particular, rats, unlike cats and monkeys, seem to have a *Salt&Pepper* arrangement in V1 (Girman et al., 1999). Thus, we predict that their connection function should belong to the *Salt&Pepper* region of the phase diagram (Figure 4A).

Experiments in tree shrew (Bosking et al., 1997) and cat V2 (Shmuel and Grinvald, 2000) show both *Pinwheel* and sizable *Icecube* regions. We predict that this should be reflected in different shapes of the connection function in these regions (Figure 4A). Our predictions regarding connection functions can be tested with experimental techniques used by Roerig and Kao (1999) and Yousef et al. (1999).

Differences in intracortical connectivity may reflect differences in visual processing between species or within the visual field of the same animal. Therefore, the map structure may be related to the statistics of natural stimuli. A similar question was addressed in the recent

work of Sharma et al. (2000) spanning different sensory modalities.

It is possible that the layout of cortical maps is preset by evolution before any visual experience. It is also likely that intracortical circuitry may be affected in the course of development by manipulating the statistics of external inputs. This approach was used to demonstrate that kittens raised in a vertically striped environment have larger cortical area devoted to neurons with vertical-preferred orientation (Sengpiel et al., 1999). Similarly, we propose that raising kittens equipped with goggles containing strong lenses (or filtering out high spatial frequency harmonics some other way) should flatten the connection function. If the appearance of the map reflects wiring optimization implemented by experience-dependent (rather than experience-independent) developmental rules, then we would expect smaller density of pinwheels.

Interaction with Other Maps

The connection function in our model is independent of other features represented by cortical neurons such as retinotopy and ocular dominance. Thus, we assume that the coupling between the orientation preference map and other maps is weak. Indeed, variability in the ocular dominance maps and discontinuities in the retinotopy do not affect the orientation preference map in ferrets (White et al., 1999). Although coupling between different maps has been reported in monkeys (Bartfeld and Grinvald, 1992; Blasdel, 1992) and cats (Crair et al., 1997; Das and Gilbert, 1997; Hubener et al., 1997), the qualitative appearance of orientation maps in these animals is similar to ferret, implying that this coupling is weak and does not affect the appearance of orientation maps significantly. This is also supported by observations of qualitatively similar orientation map in tree shrews (Bosking et al., 1997), which lack ocular dominance patterns altogether. The simplicity of our model allows us to explore the parameter space fully and to make predictions about anatomically measurable connection functions.

The dependence of the intracortical connectivity on stimulus parameters other than orientation, such as retinotopy, is not completely clear at the moment. One possible scenario is that cells with close receptive field positions (RFP) are connected. Then, in case of significant scatter of RFP (Hubel and Wiesel, 1974; Albright et al., 1984), our approach is rigorously valid. Because neurons with different RFP are intermixed in the same iso-orientation column, one can find as many close RFP neurons as needed by connecting to any cortical column in the vicinity. In this case, orientation preference map is completely decoupled from the retinotopic map. However, if scatter is not large (Das and Gilbert, 1997; Hetherington and Swindale, 1999), then retinotopic and orientation preference maps should be coupled within the wire length minimization approach. In an alternative scenario, connections between neurons may depend on the similarity of the spatial phase of their receptive fields (SPRF), as strongly indicated by DeAngelis et al. (1999). Then, due to the presence of significant scatter in the SPRF within the same cortical column (DeAngelis et al., 1999), coupling between the orientation preference map and the SPRF map is expected to be weak within our model. Coupling between orientation and retinotopic maps should be even weaker. Since the dependence of the cortical connectivity on parameters other than orientation is not clear at the moment, we postpone the treatment of the interaction between different cortical maps until more experimental evidence is available.

Relationship to Other Models

Many models of orientation maps rely on the principle of uniform coverage, i.e., complete representation of all parameters of the visual stimuli. Recently, the importance of this principle was highlighted by Swindale et al. (2000). However, the principle of uniform coverage by itself cannot explain the appearance of cortical maps. Indeed, imagine taking a map optimized for coverage and scrambling it, while keeping neuronal connections and neuronal preferred stimuli fixed. The circuit will stay the same and, hence, optimized for coverage. But the map will have a completely different structure. Therefore, another principle is needed to explain map structure. Several authors pointed out that this principle might be continuity (Hubel and Wiesel, 1977; Swindale, 1996), which requires smooth change in neuronal response properties between nearby neurons. Because the likely motivation for continuity is wire length minimization (Swindale, 1996), our theory is complementary to Swindale et al. (2000).

The structure of orientation maps has probably evolved to optimize both coverage and wire length. An example of such optimization is dimension reduction approach. However, the relative importance of the two principles is not clear. Our work shows that a single principle of wire length minimization is enough to explain both singularities in orientation maps and interspecies variability. Because our approach does not invoke the second principle, it has an advantage of being more parsimonious (Occam's razor). Future work should address the interplay between the principles of uniform coverage and wire length minimization.

Most of the existing developmental models rely on neuronal activity for map formation. Recently, however, the role of activity has been questioned (Crowley and Katz, 1999; Crowley and Katz, 2000), thus challenging the assumptions of developmental models. Because of the teleological nature of our approach, it bypasses the question of developmental mechanisms and is, therefore, immune to the outcome of the controversy on the role of activity in map formation. Whatever the developmental mechanism, it is under pressure to minimize the wiring length.

Although we left the question of developmental mechanisms outside of the scope of this paper, it is an important one. We believe that existing developmental rules should respect wire length constraints. Therefore, development can be modeled by learning rules that perform gradient descent on the cost-function expressing total wire length. In case of ocular dominance patterns, the authors have shown (Chklovskii and Koulakov, 2000) that this approach leads to learning rules that are mathematically similar to the "Mexican hat" interaction model (Swindale, 1982). An analogous calculation for the orientation preference map shows that the cost-function can be expressed in the form of two-neuron interaction simi-

lar to that in Cowan and Friedman (1991) and Swindale (1982) (see Experimental Procedures), but with the interaction kernel that depends on the relative orientations of two neurons in addition to their relative position.

Another approach to relate orientation map structure to intracortical connectivity has been proposed by Das and Gilbert (1999) and Schummers and Sur (2000). They suggested that the horizontal connections of each neuron come from a local neighborhood defined by a circle with some characteristic radius (e.g., 500 μm). This approach implicitly relies on wiring minimization hypothesis by postulating the locality of horizontal connections and is, therefore, similar in spirit to ours. An additional level of complexity arises because each neuron ends up with a different connection function. This level of complexity can be incorporated into our model by classifying neurons by their connection function in addition to different preferred orientations.

Conclusions

We find orientation preference maps that minimize the length of intracortical connections for various connection functions. We conclude that singularities in cortical maps are necessary to shorten connections between neurons with dissimilar properties for certain connection functions. We establish a link between the intracortical circuit, as characterized by the connection function, and the layout of the orientation preference map. Our theory allows one to infer the connection function from the appearance of cortical maps, thus leading to experimentally testable predictions.

Experimental Procedures

Icecube Is Optimal for Many Developmental Models

In order to model the formation of orientation preference maps, Swindale (1982) introduced learning rules for a two-dimensional orientation variable, $\theta(\mathbf{r})$. These learning rules are equivalent to a gradient decent on the following cost-function in the continuous limit (Cowan and Friedman, 1991):

$$H = -\int\int d\vec{r}\, d\vec{r}\,'\, J(\vec{r} - \vec{r}\,')\cos(\theta(\vec{r}) - \theta(\vec{r})). \quad (3)$$

Here, variable $\theta(\mathbf{r})$ represents preferred orientation at point r, J(r) gives the distribution of weights, which usually takes the "Mexican hat" form. Integration is done over the two-dimensional variable r. The above authors attempted to reproduce orientation preference maps by minimizing this cost-function.

Here we show that this cost-function is minimized by the *Icecube* layout. Therefore, within this model, pinwheels cannot exist in the optimal orientation map.

First, we rewrite the cost-function in the identical form:

$$H = -\mathrm{Re}\{\int\int d\vec{r}d\,\vec{r}\,'J(\vec{r} - \vec{r}\,')\exp(i\theta(\vec{r}) - i\theta(\vec{r}\,'))\}. \quad (4)$$

By using a Fourier transform,

$$\exp(i\theta(\vec{r})) = \sum_{\vec{k}} \exp(i\vec{k}\,\vec{r})c_{\vec{k}}$$

$$J(\vec{k}) = \int d\vec{r}J\,(\vec{r})\exp(i\vec{k}\vec{r}), \quad (5)$$

we reduce the cost-function to the following form:

$$H = -\sum_{\vec{k}} J(\vec{k})|c_{\vec{k}}|^2, \quad (6)$$

with the condition

$$\sum_{\vec{k}} |c_{\vec{k}}|^2 = 1. \quad (7)$$

This cost-function is minimized by taking

$$c_{\vec{k}} = \delta_{\vec{k},\vec{k}_0}, \quad (8)$$

with the value of k_0 corresponding to the maximum of J(k). This is equivalent to taking

$$\theta(\vec{r}) = \vec{k}\,\vec{r}, \quad (9)$$

i.e., to the *Icecube* layout.

This result shows that the "Mexican hat" cost-function is optimized by an *Icecube* layout with preferred orientation smoothly varying. Singularities in the map, such as pinwheels and fractures, are developmental defects, which can be eliminated by annihilation (Wolf and Geisel, 1998).

Salt&Pepper Is Optimal for the Uniform Connection Function

Here we prove that *Salt&Pepper* is an optimal layout for the uniform connection function. Consider a single neuron and draw a circle around it, so that the number of neurons inside the circle is equal to the total number of neurons it has to receive connections from. The total length of connections for this neuron is shortest if it receives connections from all the neurons within the circle and does not receive any from outside the circle.

To prove this, notice that any other set of connections for the given neuron can be obtained by sequentially disconnecting neurons within the circle and connecting to the ones outside. Each such step increases the total length of connections. Therefore, if each neuron receives all of its connections from all the neurons within a circle around it, such a layout minimizes the total length of connections.

In the *Salt&Pepper* layout, each preferred orientation is equally represented at every location. Therefore, connecting with neurons within a circle satisfies the uniform connection function and gives the minimal wire length.

Icecube Is Optimal for Semi-Elliptic Connection Functions

Consider a class of semi-elliptic connection functions specified by the following:

$$c(\theta) = c(0)\begin{cases}\sqrt{1 - \theta^2/\theta^2_{\max}}, & |\theta| < \theta_{\max} \\ 0, & |\theta| \geq \theta_{\max}\end{cases}. \quad (10)$$

In this case, the optimal map is *Icecube* of the appropriate periodicity. To prove this, draw a circle that includes the total number of neurons equal to the area under the connection function. Now, overlay this circle on *Icecube* layout, whose period is such that the diameter of the circle spans the range of preferred orientations equal to $2\theta_{\max}$. By connecting a neuron with every neuron in a circle around it, we satisfy the connection function and achieve the minimal wiring length. Therefore, *Icecube* is the optimal layout. The period of the *Icecube* is inversely proportional to the sharpness of the connection function.

The Model

The neurons in our model occupy a square lattice with periodic boundary conditions. We use lattices of three sizes: 30×30, 50×50, and 60×60. The preferred orientation of a neuron at each lattice site can take any value between 0 and 180 degrees. Based on the spatial distribution of preferred orientations and the connection rules, we draw connections between cells and evaluate the total connection length.

Arbitrary pattern of neuronal connections can be defined by the connection matrix M_{i-j}. By definition, the element of the connection matrix is equal to unity if the neuron number i receives connection from the neuron number $j(i, j = 1 \ldots N)$ and is zero otherwise. Here N is the total number of neurons ($N = 900$, 2500, or 3600). The connection matrices in our model are not arbitrary but satisfy constraints imposed by the connection rules. The connection rules are dictated by the function $c(\theta)$, which is defined for the discrete set of values of the difference in the preferred orientation. $\theta = 0, \Delta\theta, 2\Delta\theta, \ldots, 180^\circ - \Delta\theta$. Here the size of the angular bin $\Delta\theta = 180^\circ/$

N_θ, where $N_\theta = 15$ is the total number of angular bins. The function specifies how many connections the *i*-th neuron must receive from neurons with the preferred orientation in the range between $\theta_i + \theta - \Delta\theta/2$ and $\theta_i + \theta + \Delta\theta/2$. Here θ_i is the preferred orientation of the *i*-th neuron. Naturally, the connection function can take integer values only. Note that the connection rules specify the number of connections received by the neuron. The connection rules are therefore asymmetric. This means that even though each neuron is constrained to receive connections defined by $c(\theta)$, it does not necessarily send connections that satisfy $c(\theta)$. This is to reflect the fact that properties of a neuron are determined by received rather then by sent connections.

Having drawn the connections between neurons, we define the total connection length. To this end, we determine the distance R_{ij} between neurons *i* and *j* with periodic boundary conditions taken into account. The total connection length is then given by

$$L = \sum_{i,j=1}^{N} R_{ij} M_{i \leftarrow j}. \quad (11)$$

Numerical Minimization of the Wire Length

Connection matrix $M_{i \leftarrow j}$ is not defined uniquely by the described connection rules. For a fixed layout of the preferred orientations, one can find many connection matrices satisfying the connection rules. There is, however, a connection pattern that minimizes the total wire length. We therefore first find the minimum wire length connection matrix for a given orientation map. To this end, for each receiving connections neuron *i*, we find a subset of the entire array of neurons, which belongs to one bin specified by the connection function. More precisely, if the preferred orientation of receiving neuron is θ_i, the neurons in this subset have orientations θ in the limits $\theta_i + \Delta\theta(n - 1/2) \le \theta \le \theta_i + \Delta\theta(n + 1/2)$. Here $\Delta\theta = 180°/15$ is the width of one bin of the connection function, and *n* is the integer number labeling the bin, $-7 \le n \le 7$. Out of this subset we choose $c(n \bullet \Delta\theta)$ neurons, which are at the shortest distance to the neuron number *i*. We fill in $c(n \bullet \Delta\theta)$ entries in the matrix $M_{i \leftarrow j}$ with these neurons. We then repeat the procedure for every bin of the connection function, specified by *n*. By doing so, we both satisfy the connection rules and guarantee that the connection length is minimal for each neuron and, therefore, for the whole array, since connection patterns of different neurons are independent in our model.

Our task is, however, of a more complex nature. It is to vary the preferred orientations to find the map rendering the minimum wire length. To minimize the total wire length, the numerical algorithm attempts to change the preferred orientation of each cell in the array consecutively. More exactly, on each step of the numerical algorithm, the preferred orientation of one cell number $i (1 \le i \le N)$ is changed by the value $\delta\theta$ distributed exponentially: $\rho(\delta\theta) = \exp(-|\delta\theta|/\theta_0)/2\theta_0$. After each such attempt, the neurons are reconnected, and the wire length is recalculated. The change of the preferred orientation of the cell number *i* is then accepted or rejected based on conventional Metropolis Monte-Carlo scheme (Metropolis et al., 1953). The same procedure is then repeated for a cell number $i + 1$. After one sweep through the entire array containing N cells, the amplitude of the preferred orientation variation θ_0 is adjusted to guarantee 30% acceptance rate on the average (Koulakov and Shklovskii, 1998). To this end, we assign a new value to the parameter θ_0 given by $\theta_0^{new} = \theta_0^{old}[1 - 0.3(0.3 - Accepted/N)]$, where *Accepted* is the number of changes that are accepted after *N* attempts. The Monte-Carlo temperature is gradually annealed exponentially from 0.27 *L*/*N* to 0.0009 *L*/*N* in 10,000 sweeps through entire system steps (N × 10,000 steps). These parameters are optimized to render most consistent results for multiple restarts and to reproduce the exact solutions when available.

The calculation is first done for the arrays containing 900 and 2500 neurons. If the maps resulting from these two calculations are not consistent, the annealing procedure is repeated for 3600 neuron array. One of the three configurations, giving minimal wire length per neuron, is then accepted as the result for the given connection function. The corresponding phase (*Icecube*, *Wavy Icecube*, *Pinwheels*, or *Fractures*) is then identified by visual examination. Each annealing procedure takes about 4, 10, and 20 days to complete for 900, 2500, and 3600 neuron arrays respectively on 733 MHz Pentium III processor–based personal computer (Dell Computer Corporation, Round Rock, Texas).

Acknowledgments

This work was supported by the Sloan Foundation at Salk Institute and by the Lita Annenberg Hazen Foundation at Cold Spring Harbor Laboratory. We benefited from many helpful discussions with Chuck Stevens and suggestions from David Hubel.

Received February 18, 2000; revised December 27, 2000.

References

Ahmed, B., Anderson, J.C., Douglas, R.J., Martin, K.A., and Nelson, J.C. (1994). Polyneuronal innervation of spiny stellate neurons in cat visual cortex. J. Comp. Neurol. *341*, 39–49.

Albright, T.D., Desimone, R., and Gross, C.G. (1984). Columnar organization of directionally selective cells in visual area MT of the macaque. J. Neurophysiol. *51*, 16–31.

Allman, J.M., and Kaas, J.H. (1974). The organization of the second visual area (V II) in the owl monkey: a second order transformation of the visual hemifield. Brain Res. *76*, 247–265.

Bartfeld, E., and Grinvald, A. (1992). Relationships between orientation-preference pinwheels, cytochrome oxidase blobs, and ocular-dominance columns in primate striate cortex. Proc. Natl. Acad. Sci. USA *89*, 11905–11909.

Blasdel, G.G. (1992). Orientation selectivity, preference, and continuity in monkey striate cortex. J. Neurosci. *12*, 3139–3161.

Bonhoeffer, T., and Grinvald, A. (1991). Iso-orientation domains in cat visual cortex are arranged in pinwheel-like patterns. Nature *353*, 429–431.

Bosking, W.H., Zhang, Y., Schofield, B., and Fitzpatrick, D. (1997). Orientation selectivity and the arrangement of horizontal connections in tree shrew striate cortex. J. Neurosci. *17*, 2112–2127.

Braitenberg, V., and Braitenberg, C. (1979). Geometry of orientation columns in the visual cortex. Biol. Cybern. *33*, 179–186.

Braitenberg, V., and Schüz, A. (1998). Cortex: Statistics and Geometry of Neuronal Connectivity (Berlin: Springer-Verlag).

Buzas, P., Eysel, U.T., and Kisvarday, Z.F. (1998). Functional topography of single cortical cells: an intracellular approach combined with optical imaging. Brain Res. Brain Res. Protoc. *3*, 199–208.

Cajal, S.R.y (1999). Texture of the Nervous System of Man and the Vertebrates, Volume 1 (New York: Springer).

Cherniak, C. (1994). Component placement optimization in the brain. J. Neurosci. *14*, 2418–2427.

Chklovskii, D.B., and Stevens, C.F. (1999). Wiring optimization in the brain. In Advances in Neural Information Processing Systems-12, S.A. Solla, T.K. Leen, and K.-R. Muller, eds. (Cambridge, MA: MIT Press), pp. 103–107.

Chklovskii, D.B., and Koulakov, A.A. (2000). A wire length minimization approach to ocular dominance patterns in mammalian visual cortex. Physica A *284*, 318–334.

Cowan, J.D., and Friedman, A.E. (1991). Simple spin models for the development of ocular dominance and iso-orientation patches. In Advances in Neural Information Processing Systems-3, R. Lippmann, J. Moody, D. Touretzky, eds. (San Francisco, CA: Morgan Kaufmann), pp. 26–31.

Cowey, A. (1979). Cortical maps and visual perception: the Grindley Memorial Lecture. Q. J. Exp. Psychol. *31*, 1–17.

Crair, M.C., Ruthazer, E.S., Gillespie, D.C., and Stryker, M.P. (1997). Ocular dominance peaks at pinwheel center singularities of the orientation map in cat visual cortex. J. Neurophysiol. *77*, 3381–3385.

Crowley, J.C., and Katz, L.C. (1999). Development of ocular dominance columns in the absence of retinal input. Nat. Neurosci. *2*, 1125–1130.

Crowley, J.C., and Katz, L.C. (2000). Early development of ocular dominance columns. Science *290*, 1321–1324.

Das, A., and Gilbert, C.D. (1997). Distortions of visuotopic map match

orientation singularities in primary visual cortex. Nature *387*, 594–598.

Das, A., and Gilbert, C.D. (1999). Topography of contextual modulations mediated by short-range interactions in primary visual cortex. Nature *399*, 655–661.

DeAngelis, G.C., Ghose, G.M., Ohzawa, I., and Freeman, R.D. (1999). Functional micro-organization of primary visual cortex: receptive field analysis of nearby neurons. J. Neurosci. *19*, 4046–4064.

Durbin, R., and Mitchison, G. (1990). A dimension reduction framework for understanding cortical maps. Nature *343*, 644–647.

Erwin, E., Obermayer, K., and Schulten, K. (1995). Models of orientation and ocular dominance columns in the visual cortex: a critical comparison. Neural Comput. *7*, 425–468.

Gardner, J.L., Anzai, A., Ohzawa, I., and Freeman, R.D. (1999). Linear and nonlinear contributions to orientation tuning of simple cells in the cat's striate cortex. Vis. Neurosci. *16*, 1115–1121.

Girman, S.V., Sauve, Y., and Lund, R.D. (1999). Receptive field properties of single neurons in rat primary visual cortex. J. Neurophysiol. *82*, 301–311.

Goodhill, G.J., and Cimponeriu, A. (2000). Analysis of the elastic net model applied to the formation of ocular dominance and orientation columns. Network *11*, 153–168.

Hetherington, P.A., and Swindale, N.V. (1999). Receptive field and orientation scatter studied by tetrode recordings in cat area 17. Vis. Neurosci. *16*, 637–652.

Hubel, D.H., and Wiesel, T.N. (1974). Sequence regularity and geometry of orientation columns in the monkey striate cortex. J. Comp. Neurol. *158*, 267–293.

Hubel, D.H., and Wiesel, T.N. (1977). Ferrier lecture. Functional architecture of macaque monkey visual cortex. Proc. R. Soc. Lond. B Biol. Sci. *198*, 1–59.

Hubener, M., Shoham, D., Grinvald, A., and Bonhoeffer, T. (1997). Spatial relationships among three columnar systems in cat area 17. J. Neurosci. *17*, 9270–9284.

Kim, D.S., Matsuda, Y., Ohki, K., Ajima, A., and Tanaka, S. (1999). Geometrical and topological relationships between multiple functional maps in cat primary visual cortex. Neuroreport *10*, 2515–2522.

Koulakov, A.A., and Shklovskii, B.I. (1998). Charging spectrum and configurations of a Wigner crystal island. Phys. Rev. B *57*, 2352–2364.

Lee, D.K., Itti, L., Koch, C., and Braun, J. (1999). Attention activates winner-take-all competition among visual filters. Nat. Neurosci. *2*, 375–381.

LeVay, S., and Gilbert, C.D. (1976). Laminar patterns of geniculocortical projection in the cat. Brain Res. *113*, 1–19.

Malonek, D., Tootell, R.B., and Grinvald, A. (1994). Optical imaging reveals the functional architecture of neurons processing shape and motion in owl monkey area MT. Proc. R. Soc. Lond. B Biol. Sci. *258*, 109–119.

Metropolis, N., Rosenbluth, A.W., Rosenbluth, M.N., and Teller, A.H. (1953). Equation of state calculations by fast computing machines. J. Chem. Phys. *21*, 1087–1092.

Mitchison, G. (1991). Neuronal branching patterns and the economy of cortical wiring. Proc. R. Soc. Lond. B Biol. Sci. *245*, 151–158.

Nelson, M.E., and Bower, J.M. (1990). Brain maps and parallel computers. Trends Neurosci. *13*, 403–408.

Obermayer, K., and Blasdel, G.G. (1997). Singularities in primate orientation maps. Neural Comput. *9*, 555–575.

Peters, A., and Payne, B.R. (1993). Numerical relationships between geniculocortical afferents and pyramidal cell modules in cat primary visual cortex. Cereb. Cortex *3*, 69–78.

Rao, S.C., Toth, L.J., and Sur, M. (1997). Optically imaged maps of orientation preference in primary visual cortex of cats and ferrets. J. Comp. Neurol. *387*, 358–370.

Roerig, B., and Kao, J.P. (1999). Organization of intracortical circuits in relation to direction preference maps in ferret visual cortex. J. Neurosci. *19*, RC44.

Schummers, J., and Sur, M. (2000). Rules of functional connectivity in primary visual cortex. In Society for Neuroscience Annual Meeting (New Orleans, LA).

Sengpiel, F., Stawinski, P., and Bonhoeffer, T. (1999). Influence of experience on orientation maps in cat visual cortex. Nat. Neurosci. *2*, 727–732.

Sharma, J., Angelucci, A., and Sur, M. (2000). Induction of visual orientation modules in auditory cortex. Nature *404*, 841–847.

Shmuel, A., and Grinvald, A. (1996). Functional organization for direction of motion and its relationship to orientation maps in cat area 18. J. Neurosci. *16*, 6945–6964.

Shmuel, A., and Grinvald, A. (2000). Coexistence of linear zones and pinwheels within orientation maps in cat visual cortex. Proc. Natl. Acad. Sci. USA *97*, 5568–5573.

Swindale, N.V. (1982). A model for the formation of orientation columns. Proc. R. Soc. Lond. B Biol. Sci. *215*, 211–230.

Swindale, N.V. (1996). The development of topography in the visual cortex: a review of models. Network: Computation in Neural Systems *7*, 161–247.

Swindale, N.V., Matsubara, J.A., and Cynader, M.S. (1987). Surface organization of orientation and direction selectivity in cat area 18. J. Neurosci. *7*, 1414–1427.

Weliky, M., Bosking, W.H., and Fitzpatrick, D. (1996). A systematic map of direction preference in primary visual cortex. Nature *379*, 725–728.

White, L.E., Bosking, W.H., and Fitzpatrick, D. (1999). Visuotopic discontinuity at the V1/V2 boarder without disruption of the map of orientation preference in ferret visual cortex. In Society for Neuroscience Annual Meeting (Miami, FL).

Wolf, F., and Geisel, T. (1998). Spontaneous pinwheel annihilation during visual development. Nature *395*, 73–78.

Yousef, T., Bonhoeffer, T., Kim, D.S., Eysel, U.T., Toth, E., and Kisvarday, Z.F. (1999). Orientation topography of layer 4 lateral networks revealed by optical imaging in cat visual cortex (area 18). Eur. J. Neurosci. *11*, 4291–4308.